Acta Radiologica

Draft Manuscript for Review

A comparison of longitudinal and lateral range for protons traversing complex media using GATE, MCNP6 and FLUKA Monte Carlo simulations

Journal:	*Acta Radiologica*
Manuscript ID	Draft
Manuscript Type:	Original Article
Keyword:	Monte Carlo, GATE, MCNP6, FLUKA, proton, range

A comparison of longitudinal and lateral range for protons traversing complex media using GATE, MCNP6 and FLUKA Monte Carlo simulations

Abstract

Purpose: To compare the three Monte Carlo (MC) codes GATE/Geant4, MCNP6 and FLUKA by assessing their agreement on proton range, beam straggling, and the fraction of primary protons lost to nuclear interactions in homogeneous materials and in a proton tracking detector assembly.

Material and Methods: The mean projected range, range straggling and beam spreading of monoenergetic protons with energies varying between 50 and 230 MeV are simulated using the three MC codes "Geant4 Application for Emission Tomography" (GATE), "Monte Carlo N-Particle" (MCNP6) and "FLuktUierende KAskade" (FLUKA) as they propagate and stop inside a homogeneous water and aluminium phantom, and in a proton tracking detector assembly, representing a realistic calorimeter model for proton CT purposes.

Results: *Mean projected range deviation* of all three MC codes agree to within ± 1σ from each other, i.e. within expected range straggling. *Range straggling* show a discrepancy of up to 12.7% between the MC codes at high energies, but matches the applicable experimental data from water and aluminium. *Beam straggling* show some discrepancies between the different codes, while the *fraction of nuclear interactions* show good agreement between all MC codes and experimental data.

Conclusion: All three MC codes report good agreement for ranges and range straggling with each other and experimental data from PSTAR. The implemented physics packages, with their associated models, simulation parameter settings and material definitions are however important aspects when performing MC simulations, both during the setups, executions and in interpretation of the results from the simulations.

Introduction

The MC simulation method is at present a common, powerful and versatile tool widely used in physics research where the study of interactions between ionizing radiation and matter is of importance. MC simulations are an important tool during the development and design phase of detectors due to its ability to assess the design efficiency before finalising it. In proton Computed Tomography (proton CT), a calorimeter detector assembly applied for tracking individual protons going through a patient, and with high precision measure the energy lost so that the density of the travers matter, and also small density changes can be detected and by this produce 3D anatomical and stopping-power map of the patient for use in dose planning (1). This present work aims at comparing longitudinal and lateral range distributions obtained by three different relevant Monte Carlo simulation codes when applying a beam of high energy protons directed towards a detector, thus mimicking the required assembly for proton radiography and proton CT purposes.

A detector assembly designed with the main purpose of measuring the locations where incident high energy protons come to rest, and thus measuring their initial energy, depend upon detailed and precise knowledge about the composition and geometry of all elements in the detector assembly. This need is also coupled to the demand of sub-millimetre precision of the range of protons in the detector when the aim includes verification of correct localization of deposited dose from a proton beam.

This work will compare results from the MC codes GATE (2), MCNP6 (3) and FLUKA (4) by simulating monoenergetic protons with energies in the therapeutic span of 50 – 230 MeV as they propagate through homogeneous water and aluminium phantoms, and through a proton tracking detector assembly containing an array of different materials. Experimental data of proton range in water and aluminium from PSTAR (5) will also be included in the comparisons where applicable.

Understanding the differences between the results from each MC code will provide knowledge about the MC simulation tools and act as a quality assurance measure through cross checking of the simulation results in the initial part of this design work. For this purpose, mean projected range, range straggling and beam spreading, together with the fraction of protons lost to nuclear interactions as simulated by each of the MC codes will be analysed with the ROOT data analysis framework (6) and then compared to each other. These scoring variables represent important design figures in a proton CT system such as proton range accuracy, proton range resolution and proton track reconstruction efficiency.

In the remainder of this work, a brief description of the physics settings applied in the individual MC codes, and a presentation of the materials and geometries applied in the MC simulations will be given. This will be followed by a presentation and comparison of the results obtained by the three MC codes. In addition, the results from the MC simulations will, where applicable, be compared to existing proton range-energy tables. Finally, the results will be discussed, followed by our conclusions for this work.

Material and methods

The three MC codes GATE 7.2/Geant4 10.2.2, MCNP6.1 and FLUKA 2011.2c.5 were used to simulate monoenergetic proton beams with energies in the span between 50 – 230 MeV, in 10 MeV increments, as they propagate and come to a complete stop inside different geometries. A homogeneous water phantom, homogeneous aluminium phantom and the modelled proton tracking detector assembly were used for this purpose. The detector assembly is shown in Figure 1.

(Fig. 1)

The incident proton beam was defined to be a point source beam starting 1mm before the phantoms and consisting of 10^5 primary protons, this was kept consistent in all simulations. The physics packages chosen for each MC code, ensuring that the relevant physics processes and thresholds are accounted for in the simulations, are listed in Table 1.

Table 1. The physics packages and parameters of the applied Monte Carlo codes

MC code	Default physics package	Parameters/notes
GATE	QGSP_BIC_EMY: Using the "option 3" electromagnetic model (7),(8).	Mean Ionization potential for water set to 75 eV to match PSTAR data tables (5).
MCNP6	Cascade Exciton Model (CEM) for nuclear interactions. Vavilov straggling model for charged particle straggling(9).	Mean Ionization potential for water is automatically set to 75 eV by MCNP6, otherwise, Bragg additivity is used to calculate its value for mixtures and compounds (10,11).
FLUKA	PRECISIO (4)	Particle transport threshold set at 100 keV. Mean Ionization potential for water manually set to 75 eV.

For GATE, the physics builder list QGSP_BIC_EMY is applied as recommended for MC simulations in proton therapy and proton imaging due to a variable maximum allowed simulation step size decreasing towards the Bragg Peak, and a high resolution binning of the pre-calculated stopping power tables (7),(8). In MCNP6, nuclear interactions were modelled using the Cascade Exciton Model (CEM) 03.03 which is the recommended model for nuclear interactions (3). Use of tabulated cross-sectional data was turned off and nuclear interactions were treated using only interaction models. The default Vavilov model for charged particle straggling was used and for multiple scattering, the default FermiLab angular deflection model with Vavilov straggling (9) was used. It should be noted that all simulations using MCNP6 were run in the "proton-only" mode, thus ignoring the transport of all secondary particles other than protons. For FLUKA the predefined physics setting "PRECISIO" is recommended for precision simulations with respect to transport thresholds and activation of processes as detailed in the FLUKA manual (4). It is important to note that a manual adjustment of the ionization potentials for the different materials is possible in both GATE and FLUKA, whereas changing the automatically set ionization potentials in MCNP6 requires re-compilation of the code (10).

The homogeneous water and aluminium phantoms were defined to have a cross sectional area of 10x10 cm^2, and a 40 cm length, thus stopping all primary protons with energies up to 230MeV. The geometry and material definition of the individual layers in the detector geometry is described in Table 2.

Table 2. Description of the geometry representing the proton tracking detector assembly. A single layer is modelled as subsequent 10x10cm^2 slabs of each of the materials listed below. This is repeated 30 times to obtain the complete detector geometry.

Slab name	Material	Materials – detailed	Density [g/cm^3]	Thickness
Absorber	Aluminium	100% Al	2.69	2 mm
PCB Glue	Silver glue	100% Ag	5.25	40 µm
PCB	Quartz epoxy	15.02% H; 14.24% C; 39.1% O; 18.36% Si; 13.69% Cu	3.57	160 µm
Chip glue	Silver glue	100% Ag	5.25	40 µm
Passive chip	Silicon	100% Si	2.33	106 µm
Active chip	Silicon	100% Si	2.33	14 µm
Air gap	Air	75.5268% N; 23.1781 O; 1.2827 Ar; 0.0124 C	0.00129	170 µm
Filler absorber	Aluminium	100% Al	2.69	300 µm
Filler glue	Superglue	38.45% C; 38.45% H; 15.38% O;	1.10	70 µm

		7.69% N		
Absorber	Aluminium	100% Al	2.69	2 mm
Air gap between layers	Air	75.5268% N; 23.1781% O; 1.2827% Ar; 0.0124% C	0.00129	75 µm

This detector setup, with a final cross-sectional area of 10x10 cm^2 and 15 cm in length, ensures that approximately all protons with energies up to 210 MeV will stop inside the detector.

The final coordinates of all primary protons that stop inside the phantoms and in the detector assembly were subsequently stored, essentially giving the range of each individual proton in their respective geometries. The distribution of ranges was subsequently analysed in ROOT through a Gaussian fitting procedure to obtain the mean projected range of the proton beam. The mean projected ranges in water and aluminium were then compared to the Stopping-power and range tables for protons (PSTAR) range-energy database (5), and the respective range deviations were calculated. For the detector geometry, the range deviation is calculated as the difference from the average results from the three MC codes.

The range straggling, defined as the standard deviation of the range distribution, is obtained from and compared between the three MC codes, and in the case of the water and aluminium phantoms, also to tables of experimental data from protons in different materials listed in Janni (12).

As detailed in the work done by Makarova et al. (13), the transverse beam spread is calculated as the root mean square (RMS) value of the lateral distribution of the proton Bragg Peaks positions (σ_x), divided by the corresponding proton range.

The fraction of nuclear interactions was found in the results of each MC simulation by counting the total number of primary protons undergoing nuclear interactions in the geometry. Protons undergoing inelastic interactions are identified with different tags in the output of different MC codes. The total number of nuclear interactions was stored and the ratio between this number and the total number of primary protons in the simulated beam gave the fraction of nuclear interactions, this was then compared with the experimental data from Janni (12) where applicable. A rule-of-thumb is that approximately 1% of the protons undergo nuclear interactions per cm of water, or 1% per cm Water Equivalent Thickness (WET) when applying materials other than water (14).

Results

Values for ranges, range straggling and beam spread were obtained through simulations with the three MC codes for three different geometries. Table 3 lists the measured ranges of some selected initial primary proton energies simulated in the MC simulations and collected from PSTAR (5).

Table 3. Measured MC ranges and experimental data for 50, 100, 150 and 230 MeV primary proton energies in the water phantom, aluminium phantom and detector assembly as simulated in each of the MC codes.

Material	Energy [MeV]	GATE [mm]	MCNP6 [mm]	FLUKA [mm]	PSTAR (5) [mm]
Water	50	22.2	22.2	22.2	22.2
	100	77.0	76.8	76.0	77.1
	150	157.3	156.9	157.3	157.6
	230	328.7	327.4	328.6	329.1
Aluminium	50	10.8	10.8	10.9	10.8
	100	37.0	36.9	37.1	37.0
	150	75.0	75.0	75.3	75.1
	230	155.8	156.1	156.3	156.0
Detector assembly	50	11.1	11.1	11.1	-
	100	37.9	38.0	37.9	-
	150	76.8	76.8	77.1	-
	210	137.0	137.2	137.3	-

As is also shown in Figure 2, the mean projected range between MC codes and PSTAR display good agreement, with the *range deviation* being less than 0.52% from PSTAR in water and 0.2% in aluminium. Range deviation in the detector assembly, calculated as the deviation from the average of the ranges found the three MC codes, deviates no more than 0.1% from each other. It is noted that while FLUKA and GATE match each other well in water, MCNP6 yield a larger range deviation with increasing initial proton energy.

(Fig. 2)

The obtained results of *Range straggling* for some selected primary proton energies are listed in Table 4 and full complete MC simulation results are displayed in Figure 3.

Table 4. Results for MC range straggling and experimental data for 50, 100, 150 and 230 MeV primary proton energies in the water phantom, aluminium phantom and detector assembly as simulated in each of the MC codes.

Material	Energy [MeV]	GATE [mm]	MCNP6 [mm]	FLUKA [mm]	Janni (12) [mm]
Water	50	0.28	0.28	0.30	0.28
	100	0.87	0.95	0.92	0.91
	150	1.70	1.92	1.80	1.79
	230	3.36	3.84	3.60	3.45*
Aluminium	50	0.16	0.15	0.17	0.14
	100	0.45	0.47	0.48	0.44
	150	0.87	0.93	0.92	0.86
	230	1.73	1.78	1.81	1.64*
Detector assembly	50	0.16	0.14	0.17	-
	100	0.48	0.42	0.49	-
	150	0.88	1.02	0.98	-
	210	1.53	1.64	1.60	-

*Range straggling data from Janni (12) is for 225 MeV protons.

All applied MC codes are showing a relatively similar amount of range straggling, with a maximum difference between the MC codes of 12.7% in water and 4.9% in aluminium. This tendency is also observable in the results for the detector assembly, where the largest deviation between the average and individual MC codes is about 6.4%.

(Fig. 3)

The beam spread displayed in Figure 4, shows an agreement between MCNP6 and FLUKA, with GATE reporting an overall lower amount of beam spreading, and MCNP6 reporting a slightly higher amount of beam spread. This is confirmed by beam profiles taken from a 120 MeV proton beam incident on the water phantom as shown in Figure 4(d).

(Fig. 4)

Moreover, the fractions of primary proton undergoing nuclear interactions as calculated in the MC simulations are shown in Figure 5 for both water, aluminium and the detector geometry. For water and aluminium, the MC calculated results are compared to experimental data from Janni(12). The fraction of nuclear interactions in Figure 5 indicate that all three MC codes yield an almost equal amount of nuclear interactions in

the simulated proton beams, with no more than a 0.02% deviation between the MC codes.

(Fig. 5)

Discussion

The objective of this study has been to compare results for simulations of range distributions for protons traversing different materials obtained with the three MC codes GATE, MCNP6 and FLUKA by assessing their agreement on projected proton range, range straggling, beam spread, and also the fraction of protons lost from the primary beam in nuclear interactions. These parameters were compared in situations with protons traversing homogeneous water and aluminium phantoms and in a proton tracking detector assembly. The MC results were also compared with PSTAR (5) data for particle range in water and aluminium. The main motivation for performing these comparisons were to achieve detailed knowledge about the MC codes as a quality assurance tools in the initial design work of a proton CT detector for which experimental data is presently unavailable. These scoring variables represent important design figures in a proton CT system. Validation of the MC simulation results based on comparisons with experimental data, where available, show that the each of these three MC codes may be used as a validation tool for a proton tracking detector in development phase, as all three MC codes report similar ranges and range straggling and in agreement with range from the PSTAR (5) database.

There are however important aspects to be aware of in the planning of simulation setups and during interpretation of the results as also mentioned in a topical review article on the role of range uncertainties in MC by Paganetti (15). Awareness should be placed on how different MC codes handle the implementation of their respective models for physics interactions, which can be done either by theoretical models or through interpolation of experimental data depending on the energy region that is studied. In this regard, certain physics models and MC code packages can be better suited to describe a clinical proton beam than others. Table 1 in the material and methods chapter and references therein lists the recommended packages used in this work.

User defined settings that are easily changed in one MC code, can be difficult or impossible to change in others. As is seen in Figure 2(a) for the range deviation in water, MCNP6 diverges from the other codes with increasing initial energy. A potential cause for this divergence is the ionization potential (IP), which is an important process in estimating the range of protons in low Z materials (16). Five separate GATE

simulations with varying IP were performed and the resulting ranges compared to the MCNP6 range. Figure 6 shows the range deviation between MC simulations using GATE and MCNP6. It is noted**Error! Reference source not found.** that MCNP6 uses recommended values for the IP for a material from ICRU49 (17) where applicable, otherwise it uses Bragg Additivity to calculate the IP for composite materials. It should also be noted that by setting the IP of water to 73eV in GATE (instead of the ICRU49-recommended value of 75 eV), the resulting proton ranges are closer to the ranges obtained in MCNP6.

(Fig. 6)

Others have also found that the results depend significantly on user defined settings in MC simulations. Kimstrand (18) have modelled and compared transport of protons grazing a tungsten block between Geant4.8.2, FLUKA2006 and MCNPX2.4.0 and found that, while the energy spectrum of out-scattered protons agreed between codes, dose-weighted out-scatter probability was highly dependent on user-defined settings, and quantitatively the deviation between simulations could reach up to 37%.

Other studies have further shown discrepancies in beam spreading between different MC codes and experimental data, with Grevillot et al. (8) reporting that GATE/Geant4 underestimates the transversal spread, attributed to the multiple scattering (MS) model applied in GATE. Mertens et al.(19) notes that MCNP6 overestimates the spread in low density and low-Z targets, suggesting inaccuracies in the scattering cross-sections as a reason for the overestimation. This behaviour can be observed in Figure 4, with GATE yielding a lower amount of beam spread than FLUKA and MCNP6.

In conclusion, while the compared MC codes show good agreement for the range of primary protons in matter, thus displaying their potential as quality assurance tools for a proton tracking detector assembly where no experimental data is currently available, still care must be taken in the planning, execution and evaluation of MC simulations. Knowledge about the limitations of the applied physical processes and models incorporated in the MC code, together with detailed, consistent and representative definitions of the involved materials and geometries, are very important for decreasing the uncertainties and increasing the overall reliability of the MC simulations.

References

1. Sadrozinski HF-W, Bashkirov V, Keeney B, et al. Toward Proton Computed Tomography. IEEE Trans Nucl Sci. 2004 Feb;51(1):3–9.

2. Geant4 Application for Emission Tomography (GATE) [Internet]. [cited 2016 Dec 20]. Available from: http://www.opengatecollaboration.org

3. Goorley JT, James MR, Booth TE, et al. Initial MCNP6 release overview-MCNP6 version 1.0. Los Alamos Natl Lab Los Alamos NM -UR-13-22934 [Internet]. 2013 [cited 2016 Dec 20];1. Available from: https://mcnp.lanl.gov/pdf_files/la-ur-13-22934.pdf

4. Ferrari A, Sala PR, Fasso A, Ranft J. Fluka: a multi-particle transport code (Program version 2011). CERN-Libr Httpfluka Web Cern Chfluka. 2005;55(99):100.

5. NIST Physics Laboratory. PSTAR - Stopping-power and range tables for protons [Internet]. [cited 2016 Dec 23]. Available from: http://physics.nist.gov/PhysRefData/Star/Text/PSTAR.html

6. Brun R, Rademakers F. ROOT — An object oriented data analysis framework. Nucl Instrum Methods Phys Res Sect Accel Spectrometers Detect Assoc Equip. 1997 Apr;389(1–2):81–6.

7. Zacharatou Jarlskog C, Paganetti H. Physics Settings for Using the Geant4 Toolkit in Proton Therapy. IEEE Trans Nucl Sci. 2008 Jun;55(3):1018–25.

8. Grevillot L, Frisson T, Zahra N, et al. Optimization of GEANT4 settings for Proton Pencil Beam Scanning simulations using GATE. Nucl Instrum Methods Phys Res Sect B Beam Interact Mater At. 2010 Oct;268(20):3295–305.

9. Mokhov NV, Striganov SI. Implementation of MARS Hadron Production and Coulomb Scattering Modules into LAHET. Los Alamos Natl Lab Los Alamos -UR-03-4264 [Internet]. 2002 [cited 2017 Jan 2]; Available from: https://laws.lanl.gov/vhosts/mcnp.lanl.gov/pdf_files/la-ur-03-4264.pdf

10. Seravalli E, Robert C, Bauer J, et al. Monte Carlo calculations of positron emitter yields in proton radiotherapy. Phys Med Biol. 2012 Mar 21;57(6):1659–73.

11. James MR. Personal Communication, Los Alamos National Library.

12. Janni JF. Energy loss, range, path length, time-of-flight, straggling, multiple scattering, and nuclear interaction probability. At Data Nucl Data Tables. 1982 Mar;27(2–3):147–339.

13. Makarova A, Gottschalk B, Sauerwein W. Comparison of Geant4 multiple Coulomb scattering models with theory for radiotherapy protons. ArXiv Prepr ArXiv161001279 [Internet]. 2016 [cited 2017 Jan 2]; Available from: https://arxiv.org/abs/1610.01279

14. Durante M, Paganetti H. Nuclear physics in particle therapy: a review. Rep Prog Phys. 2016 Sep 1;79(9):096702.

15. Paganetti H. Range uncertainties in proton therapy and the role of Monte Carlo simulations. Phys Med Biol. 2012 Jun 7;57(11):R99–117.

16. Newhauser WD, Zhang R. The physics of proton therapy. Phys Med Biol. 2015 Apr 21;60(8):R155–209.

17. Deasy J. ICRU Report 49, Stopping Powers and Ranges for Protons and Alph Particles. Med Phys. 1994 May;21(5):709–10.

18. Kimstrand P, Tilly N, Ahnesjö A, et al. Experimental test of Monte Carlo proton transport at grazing incidence in GEANT4, FLUKA and MCNPX. Phys Med Biol. 2008 Feb 21;53(4):1115–29.

19. Mertens CJ, Moyers MF, Walker SA, et al. Proton lateral broadening distribution comparisons between GRNTRN, MCNPX, and laboratory beam measurements. Adv Space Res. 2010 Apr;45(7):884–91.

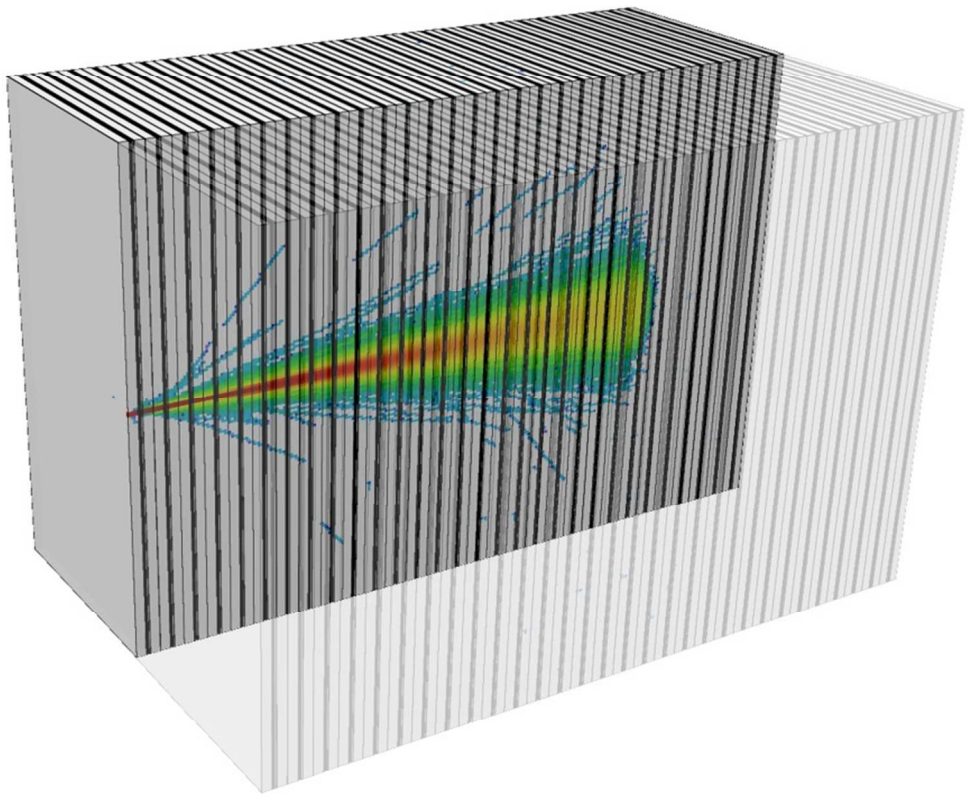

Figure 1. The proton tracking detector assembly overlaid with a MC simulated primary proton flux of 105 protons in the middle of the detector.
(Fig. 1)
118x101mm (192 x 192 DPI)

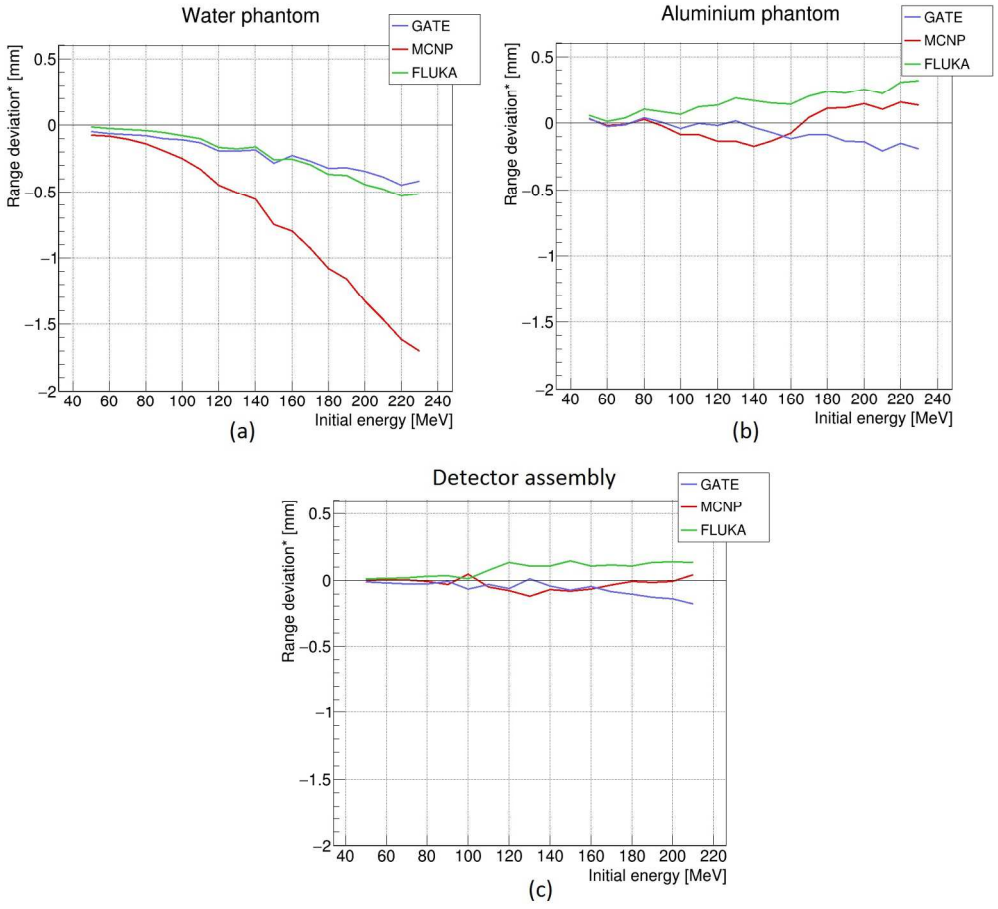

Figure 2. Results for mean range deviation shown as the deviation from PSTAR data with respect to the initial energy of the incoming primary protons in water, Figure 2(a), and aluminium, Figure 2(b). And as the range deviation from the average of the three MC in the detector assembly, Figure 2(c).
(Fig. 2)
261x241mm (192 x 192 DPI)

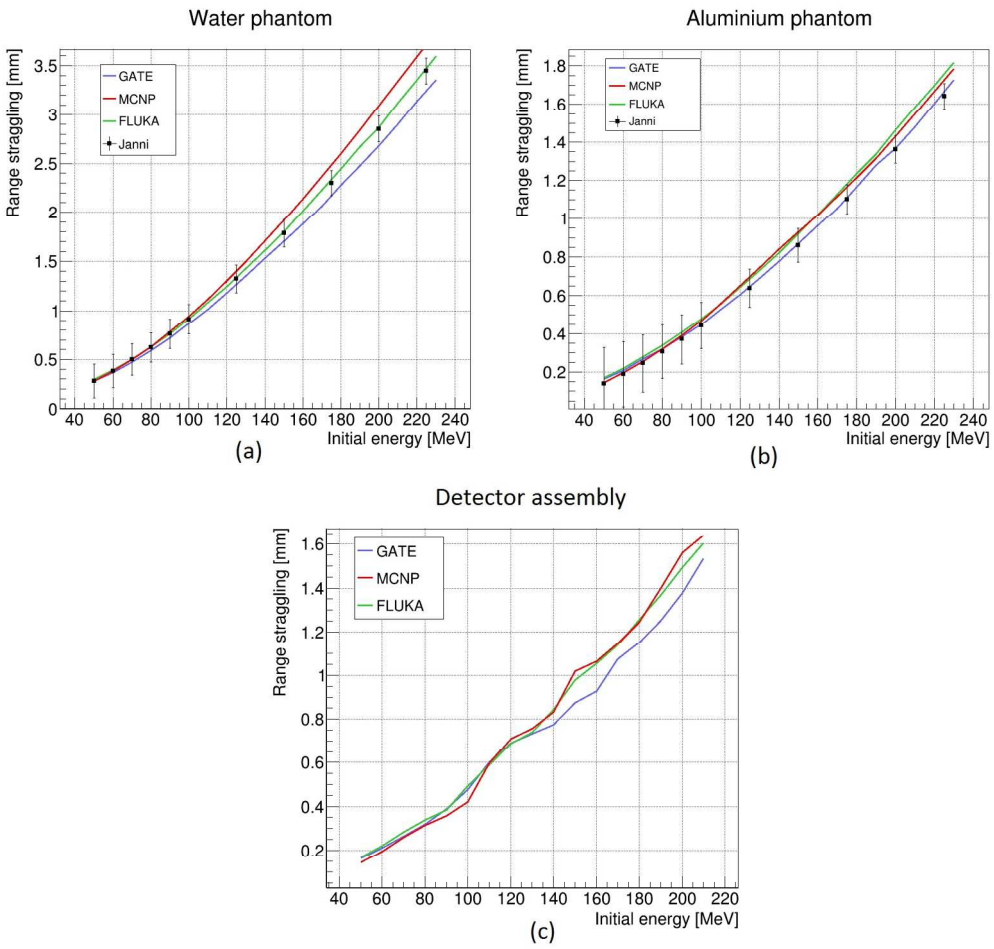

Figure 3. MC results for range straggling in water, Figure 3(a), aluminium, Figure 3(b), and the detector assembly, Figure 3(c), for the three different MC codes. The simulation results are compared with experimental data where available.
(Fig. 3)
251x241mm (192 x 192 DPI)

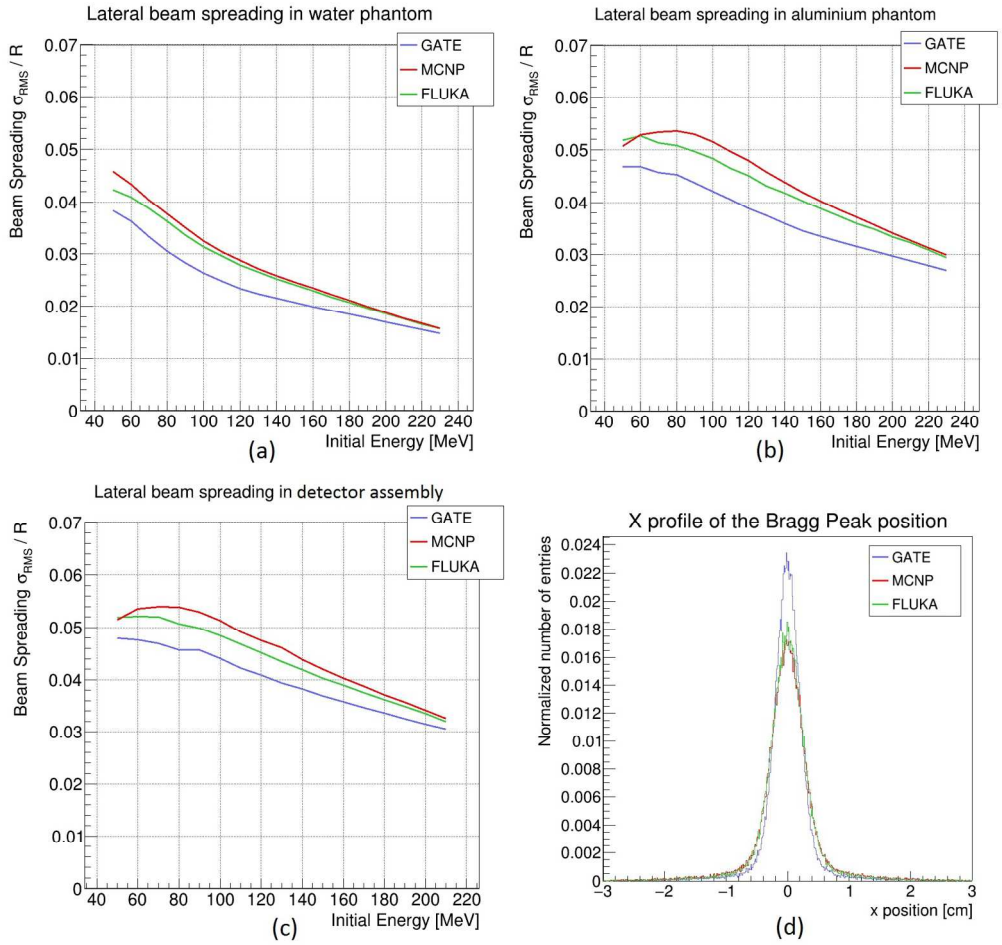

Figure 4. MC simulation results: Calculated beam spread in water, Figure 4(a), aluminium, Figure 4(b) and the detector assembly, Figure 4(c). Figure 4(d) display the lateral (in x) profile of the Bragg Peak for the three MC codes.
(Fig. 4)
247x236mm (192 x 192 DPI)

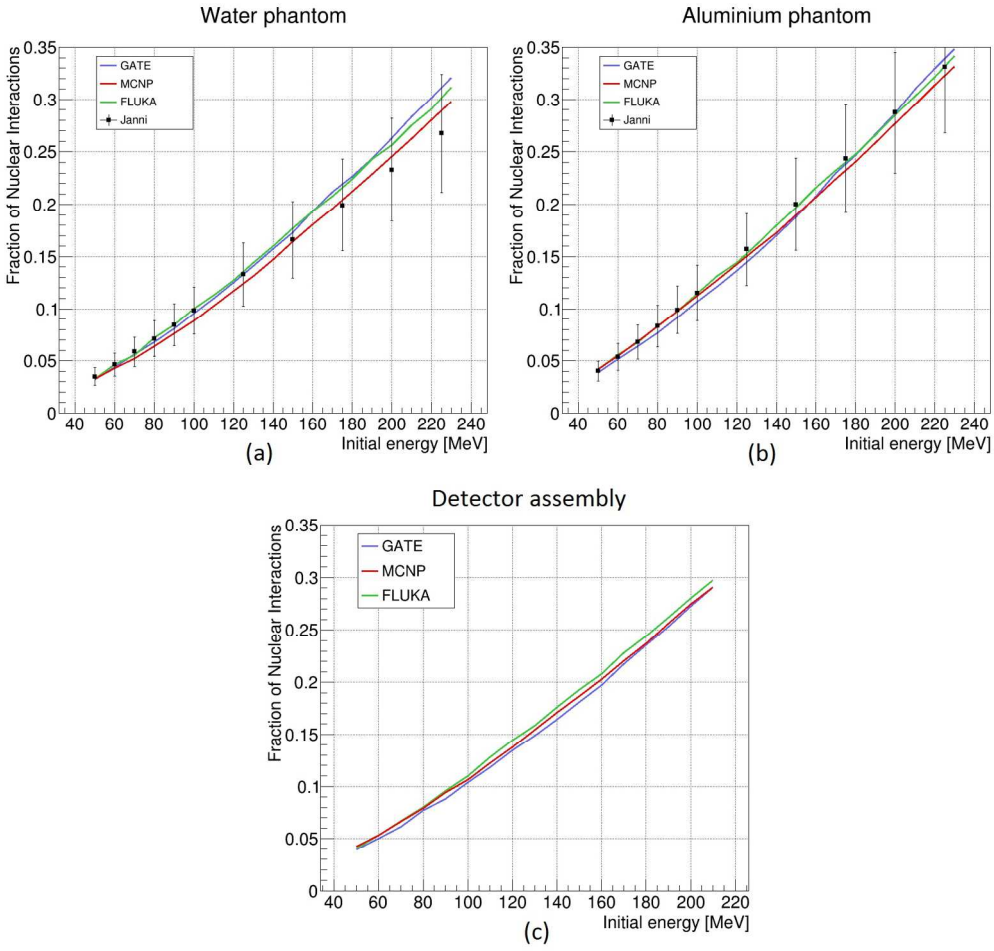

Figure 5. MC simulation results: The fraction of nuclear interactions in water, Figure 5(a), aluminium, Figure 5(b) and in the detector assembly, Figure 5(c).
(Fig. 5)
247x236mm (192 x 192 DPI)

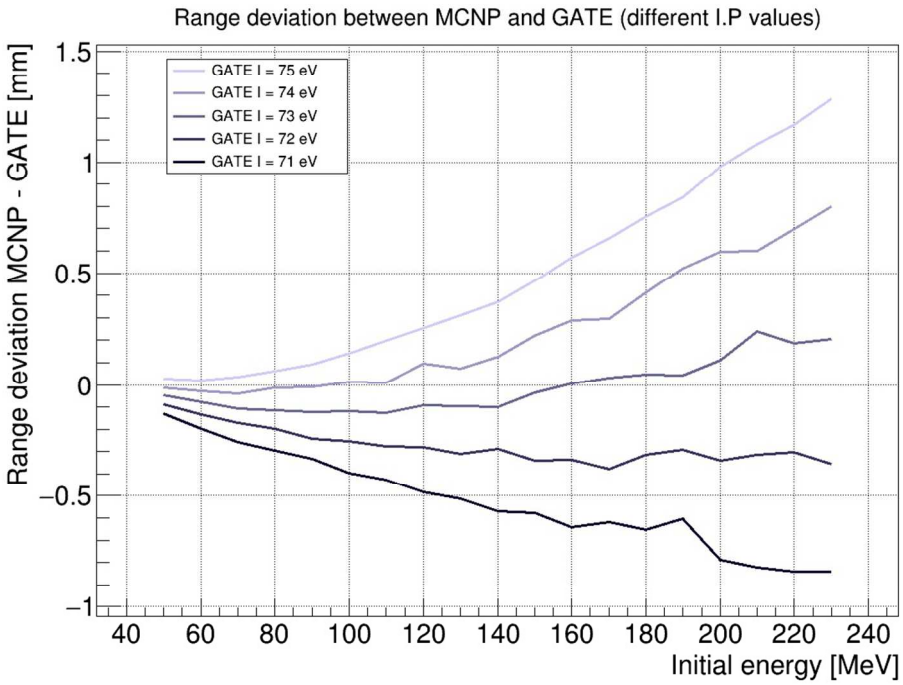

Figure 6. Range deviation between MCNP6 and five separate GATE simulation sets with increasing energies, each performed with a different IP in the 71-75eV span for each initial energy of the primary protons.
(Fig. 6)
158x113mm (192 x 192 DPI)